Am J Cancer Res 2021;11(4):1247-1266
www.ajcr.us /ISSN:2156-6976/ajcr0124694

Original Article

Cordycepin inhibits the proliferation of malignant peripheral nerve sheath tumor cells through the p53/Sp1/tubulin pathway

Ming-Jen Lee[1,2], Jen-Chieh Lee[3], Jung-Hsien Hsieh[4], May-Yao Lin[1], I-An Shih[1], Huey-Ling You[1], Kai Wang[5]

[1]Department of Neurology, National Taiwan University Hospital, National Taiwan University College of Medicine, Taipei, Taiwan, ROC; [2]Department of Neurology, National Taiwan University Hospital, Yunlin Branch, Yunlin, Taiwan, ROC; [3]Department and Graduate Institute of Pathology, National Taiwan University Hospital, National Taiwan University College of Medicine, Taipei, Taiwan, ROC; [4]Department of Plastic Surgery, National Taiwan University Hospital, National Taiwan University College of Medicine, Taipei, Taiwan, ROC; [5]Institute for Systems Biology, Seattle, Washington, USA

Received October 21, 2020; Accepted January 14, 2021; Epub April 15, 2021; Published April 30, 2021

Abstract: Neurofibromatosis type 1 (NF1) is one of the most common hereditary neurocutaneous disorders. In addition to skin pigmentation and cutaneous neurofibroma, some patients developed the plexiform neurofibroma since birth. Plexiform neurofibroma has abundant Schwann cells, fibroblasts, mast cells, blood vessels, and connective tissues, which increases the risk of developing a malignant peripheral nerve sheath tumor (MPNST). MPNST is a highly invasive cancer with no effective therapeutic agent. Cordycepin or 3'-deoxyadenosine is an extract from cordyceps militaris, which has been reported as an anti-inflammation and anti-tumor agent. Herein, we evaluated cordycepin's anti-proliferative effect on MPNST cell lines both *in vitro* and *in vivo*. Cordycepin inhibited the MPNST cell growth with an arrest of cell cycle at G2/M and S phases. The administration of naringin and pentostatin, inhibitors for adenosine deaminase (ADA), enzyme responsible for cordycepin degradation, did not show a synergistic effect in MPNST cells treated with cordycepin. However, the combined treatment enhanced the decrease of tumors in xenograft mouse model. Immunoblotting showed a decreased level of p53 protein in all MPNST cell lines, but S462TY cells. After cordycepin treatment, the levels of ERK, survivin, pAKT, and Sp1 proteins also decreased. The level of tubulin, but not actin or GAPDH, decreased in a dose-dependent manner. The microtubule network which is composed of tubulins was markedly decomposed in those treated MPNST cells. To elucidate the epigenetic control of transcription, ChIP-qPCR assay of the Sp1 and tubulin promoter regions revealed decreased Sp1 binding. The incorporation of 3'-doexyadenosine is detrimental for the process of poly(A) tail elongation. The poly(A) tail length assay showed the tail length in Sp1 and tubulin transcripts decreased in the treated cells. Nevertheless, the administration of SP1 protein to the treated cells could not rescue them completely. Furthermore, the p53-knocked-down cells (S462TY) where the expression of both p53 and Sp1 was suppressed, were vulnerable to cordycepin. The p53 protein could ameliorate the effect. In summary, cordycepin is effective to inhibit the growth of MPNST, probably through the pathway of p53/Sp1/tubulin.

Keywords: Cordycepin, MPNST, ChIP, poly(A) tail length, p53/Sp1/tubulin

Introduction

Neurofibromatosis type 1 (NF1) is a common autosomal dominant neurological disorder with a prevalence rate of 1 in 3500 individuals. Besides the skin pigmentation such as cafe-au-lait spots, another hallmark for NF1 patients is the growth of benign neurofibromas with Schwann cells being the chief component. Cutaneous neurofibromas usually appear in late childhood and grow relentlessly throughout life, especially during puberty and pregnancy [1, 2]. However, about one in four NF1 patients develop one or more plexiform neurofibroma(s) (PN) [3]. The PN typically appears during early childhood, which involves the entire nerve with abundant collagen tissues and blood vessels [3]. The tumor raises a particular concern as they can undergo malignant transformation to a sarcoma, *i.e.*, malignant peripheral nerve

sheath tumor (MPNST) [4]. NF1 patients have a 5-13% lifetime risk to develop an MPNST; the risk is even higher for those with a large plexiform neurofibroma [4, 5]. The MPNST is highly invasive and resistant to conventional radio- and chemotherapies. Thus, developing an armamentarium which could effectively inhibit the growth of MPNST is urgently needed.

A growing body of evidence shows that cancer is caused by the imbalance between the progression of cell cycle and programmed cell death [6]. Thus, most of the anticancer therapeutics exert an anti-proliferative activity through cell cycle arrest with subsequent induction of apoptosis [7, 8]. For example, the cytotoxic nucleoside analog cordycepin (3'-deoxyadenosine), one of the first chemotherapeutic agents proposed for cancer treatment, is the main constituent of the mycelia of *Cordyceps militaris* identified in 1950 [9]. In the mouse model, cordycepin has been shown to reduce melanoma and lung adenocarcinoma tumor size [10]. Besides anti-cancer activities, cordycepin exhibited antiviral and antifungal activities [11-13]. Some studies showed that Cordycepin possessed anti-inflammatory, antithrombotic, and antiadipogenetic activities as well [14-17]. Cordycepin is an adenosine analog, differing from the latter by lacking the hydroxy group at the 3' position of the ribose moiety, and inhibits mRNA synthesis and polyadenylation [18]. The poly(A) tail derived through polyadenylation is essential for the stability and nuclear export of mRNA [19]. Further study of cordycepin with human epithelial endometriotic cells also demonstrated its ability to inhibit the cell proliferation and induce apoptosis through the inhibition of mRNA polyadenylation [20].

Adenosine deaminase (ADA) is responsible for the deamination of adenosine to inosine, which is further degraded into hypoxanthine. Degradation of cordycepin (3'-deoxyadenosine) is mediated and catalyzed also by ADA. Thus, ADA inhibitors such as pentostatin and naringin is usually administered in combination with cordycepin in *in vitro* or *in vivo* anticancer studies [21, 22]. In this report, we evaluated the effect of cordycepin on MPNST cells in culture and xenograft animal models. In addition, we examined the synergistic effect on MPNST cells when combined the cordycepin treatment with ADA inhibitors.

We also explore the molecular mechanisms and the epigenetic modifications associated with the anti-tumor effect of cordycepin. The treatment of cordycepin reduced the survival of MPNST cells both *in vivo and in vitro*. The levels of tubulin, but not actin or GAPDH decreased significantly in those treated cells. To explore the regulatory control of tubulin expression, the binding of transcription factors Sp1 and p53 have been evaluated. In addition, we also assessed the involvement of histone acetylation and changes of poly(A) tail length in cordycepin induced cell death.

Materials and methods

Cell culture

The MPNST cell lines used in this study have been reported before [23]. The S462TY cell line was a kind gift from Dr. Timothy Cripe (Nationwide Children's Hospital Columbus, OH) [24]. All the other MPNST cell lines were gifted from Dr. Nancy Ratner (Cincinnati Children's Hospital, Cincinnati OH) and grown as described [24]. The primary human Schwann cells (HSC) were purchased from ScienCell (ScienCell Research Laboratory, Carlsbad, CA, USA) and grown on Poly-L-Lysine and laminin coated tissue culture plates. The cells were grown in DMEM medium according to ATCC's instruction. In brief, the cells were maintained in medium with 20% FBS, 7 ng/ml HRG (Heregulin) (R&D Systems), 2 μM Forskolin (EMD) and 2.5 μg/ml Insulin (GIBCO, Thermo Fisher Scientific™, Waltham, MA). The cells were kept in a humid incubator at 37°C with 5% CO_2. Primary cells from the benign cutaneous neurofibroma were also subjected to the treatment of cordycepin. The use of human samples in this study was approved by the Institutional Review Board of National Taiwan University Hospital.

Cell proliferation assay

To evaluate the cell death after treatment, the cells were seeded at a density of 1.5×10^5 cells/mL onto 96-well plates and grown overnight. Cordycepin and naringin were dissolved in dimethyl sulfoxide (DMSO). The cells were treated with different concentrations of cordycepin or naringin for 24 h before the assay. The control group was treated with 0.025% of DMSO. The cell viability was evaluated by the colorimetric assay. In brief, 7.5 μL of 5 mg/mL

MTT [3-(4, 5-dimethylthiazol-2-yl)-2, 5-diphenyl tetrazolium bromide] was added to each well, and cells were incubated for 3.5 h at 37°C. After incubation, 75 μl of DMSO was added to each well for 20 min at room temperature to dissolve the precipitates. The absorbance was recorded by a microplate reader at a wavelength of 590 nm.

Flow cytometry cell cycle analysis

The treated cells were resuspended and washed with ice-cold PBS before fixation with 70% of ethanol at -20°C for one hour. The cells were centrifuged at 300 × g for 5 min and then incubated with 0.1% TWEEN20, 0.2 mg/dL of RNase A and 20 μg/mL of propidium iodide at room temperature for 30 min in dark. The 35 μm of nylon mesh was used to filter the cells before FACS analysis (FACSVerse, BD Bioscience, USA). At least 50,000 events per sample were acquired from each of the MPNST cells.

Western blotting assays

The samples were harvested and sonicated in RIPA lysis buffer (50 mM Tris HCl pH 7.6, 150 mM NaCl, 1% NP-40, 1% sodium deoxycholate, 0.1% SDS) to extract the proteins. The bicinchoninic acid (BCA) method was used to determine the protein concentration. For immunoblotting, the proteins were denatured by boiling at 100°C for 5 min followed by SDS-PAGE. The proteins on the gel were then transferred onto a PVDF membrane. After blocking with 5% skim milk for one hour at room temperature, the membranes were incubated with the indicated primary antibodies, including anti-AKT (1:2000, A302-065A, Bethyl Laboratories, Inc., Montgomery, TX), anti-P-AKT (1:2000, #4060, Cell Signaling Technology, Inc., Danvers, MA), anti-β-actin (1:4000, 4967S, Cell Signaling Inc.), anti-α-tubulin (1:5000, 11224-1-AP, Proteintech Group, Inc, Rosemont, IL), anti-p53 (1:2000, ab32389, Abcam plc., Cambridge, MA), anti-Sp1 (1:10000, A300-134A, Bethyl), and anti-GAPDH (1:10000, 10494-1-AP, Proteintech) antibodies, overnight at 4°C. Then, the membrane was washed with PBS containing 5% skim milk followed by incubation with horseradish peroxidase-conjugated secondary antibodies, the goat anti-rabbit IgG-HRP (#A120-101P, Bethyl, Montgomery, TX) for two hours. The protein signals were detected using the enhanced chemiluminescence method and quantified by UVP BioSpectrum 810 Imaging System (Thermo Fisher Scientific).

Confocal microscopy

The treated cells were washed with PBS twice then fixed with 4% of paraformaldehyde (PFA) for 30 min. The cell membrane was permeabilized with 0.1% of Triton X-100 for ten min. After PBS washing, the samples were blocked with 5% FBS/PBS at 4°C overnight. The antigen-antibody reaction with the primary antibody (1:400 dilution), anti-Sp1 or anti-p53 in 1% BSA/PBS were carried out at 4°C overnight. Then, the secondary antibody (1:1000, donkey anti-mouse) were applied to the cells and incubated at 4°C overnight. After washing, the samples were stained with DAPI. The confocal images were acquired with a Zeiss LSM 880 (Zeiss, Germany).

Immunofluorescence

Cells were cultured in dishes (IB-81156, Ibidi), after washing with calcium and magnesium free PBS (twice), the cells were fixed in 4% PFA for 30 min at room temperature (RT). The cells were permeabilized with 0.1% Triton X-100 (T8787, Sigma) in PBS for 10 min at RT then blocked with 5% Fetal Bovine Serum for 1 hr at RT. The primary antibody against α-tubulin (1:500, 11224-1-AP, Proteintech) in blocking buffer was added and incubated overnight at 4°C. The excess primary antibody was washed away and FITC-conjugated goat anti-rabbit (1:1000, ab6717, Abcam) antibody was added and incubated for 1 hr at RT. After washing, the cells were further stained with DAPI (1:5000, D9542, Sigma) 10 min at RT. Cells were washed with PBS and mounted with Ibidi Mounting Medium (50001, Ibidi).

Human MPNST xenograft mouse model

The 4 week old male Balb/c nude mice were obtained from the BioLASCO Experimental Animal Center (BioLASCO, Taipei, Taiwan). All animal procedures were approved by the National Taiwan University Hospital's Animal Care and Use Committee (20140041). The ST8814 cells, ~5 × 10^7, were prepared in 0.1 ml DMEM medium and mixed with 0.1 ml Corning® Matrigel (Gibco, Thermo Fisher Scientific). The mixture was injected subcutaneously on the flank of each nude mouse. The

tumor sizes were measured using calipers, and the tumor volumes were estimated (Tumor volume (mm^3)) = maximum length (mm) * (perpendicular width $(mm)^2$)/2). As soon as the tumor size reached a mean of 100-150 mm^3, the mice were subjected to injections with a total volume of 100 μl of PEG, 67 mg/kg of cordycepin, 50 mg/kg of naringin, and the combination of cordycepin and naringin. The injections were carried out three times a week for 26 days. The body weight was recorded and the tumor volume was assessed using a Vernier caliper.

Immunohistochemistry (IHC)

After the mice were sacrificed, the xenografted tumors were isolated and fixed with PFA. For immunostaininig, the sections from paraffin-embedded tissue block was deparaffinized and rehydrated. Then, the slices were immersed in 3% hydrogen peroxide for 10 min to block endogenous peroxidase followed by incubation with either anti-SP1 (1:1000, A300-134A, Bethyl) or anti-p53 (1:400 in dilution, Abcam) antibody at 4°C overnight. The FITC-conjugated goat anti-rabbit (1:1000, ab6717, Abcam) antibody was applied onto the slices then incubated at RT for 1 h. The sections were counterstained with DAPI.

Gene-specific measurement of poly(A) length

To validate the alteration on the length of poly(A) tail of individual genes, poly(A) tail length assay kit (Affymetrix, 76455, Thermo Fisher Scientific) (Bazzini et al., 2012) were used. In brief, total RNA was isolated from the treated cells. The guanosine and inosine (G/I) residues were annealed onto the 3'end of the extracted mRNA. The tailed-RNAs are reverse-transcribed using the newly added G/I tails as the priming sites. PCR amplification was performed using two primer sets: (1) a gene-specific forward and reverse primer set designed upstream of the polyadenylation site as control and (2) a gene-specific forward primer and the universal reverse primer which is provided with the kit to generate a product including poly(A) length. The gene-specific primers used in the study are as follows: *ACTB* (forward, 5'-TGCTTTCGTGTAAATTATGTAATGC-3'; reverse, 5'-CATTTTTAAGGTGTGCACTTTTATTC-3'), *TUBA1B* (forward, 5'-GAAGAAGGAGAGGAATACTAA-3'; reverse, 5'-GATGTTAATGACTTTACTTTGAG-3') and *SP1* (forward, 5'-AATCTTGTCCCTAAGTAAGTT-3'; reverser, 5'-GCTCCTTTTGTATCTTCCTTTCTT-3'). PCR products were detected by 2.5% of agarose gel electrophoresis. To observe the changes in the poly(A) length after treatment, the genescan was used and the fragment size was calculated using interpolating method. The actual poly(A) length can be calculated by the subtraction between the fragment size obtained from forward primer site to the 5'-juxta-polyadenylation reverse primer site and the fragment size from the same forward primer to the universal reverse primer site.

Promoter sequence prediction

The core binding sequence for the transcription factor (TF) Sp1 is GGGCGG and for p53 is RCWWGY. The bindings sites of Sp1 and p53 TFs have been screened in the promoter region (-1~-500 base pairs 5' of the transcriptional start site) of the candidate genes, *TUBA1A, TUBA1B, ACTB, SP1,* and *GAPDH*.

Chromatin immunoprecipitation (ChIP) assay

The ChIP assay was carried out using the Pierce Magnetic ChIP Kit (Thermo Fisher Scientific™) following the manufacturer's protocol. In brief, the cell lysate was digested with Micrococcal nuclease (MNase) and sonicated to about 400 bp chromatin fragments. The sheared chromatin was centrifuged (9000 × g) at 4°C for 5 min. Ten percent of the diluted supernatant (input) was set aside as a control template for RT-PCR. The sheared chromatin was then, immunoprecipitated with anti-Sp1 antibody and incubated overnight (Bethyl Laboratories, Montgomery, TX). Magnetic beads and magnetic separation device (Cat. #: 20-400, Merck, Darmstadt, Germany) were employed to isolate the protein/DNA complexes from the crude chromatin mixture. After elution, the DNA from immunoprecipitated samples and the inputs were recovered by phenol/chloroform. The input DNA and antibody-bound chromatin DNA were subjected to a RT-PCR using primers designed to amplify a fragment of the *TUBA1B, SP1* and *hACTB* promoters. The primer sequences for *TUBA1B* gene were 5'-CATTTCACGGTGCTTCGTC-3' and 3'-AAAGACACCGACCAGGGAAT-5', for *SP1* gene were 5'-GTCTTTTTAGGCGGACACCA-3' and 3'-GGAGGGACTTGCAGAAGAAA-5', and for *hACTB* gene were 5'-GGACATCCGCAAAGACCTGTA-3' and 5'-TGCATCCTGTCGGCAATG-3'. For quantitation, the cycles of the threshold value (C_T) of

the amplicons after real-time PCR have been counted to represent its amplified number. Using C_T value as a semi-quantitative indicator, the values of $\Delta\Delta C_T$ were compared among the cell lines to express the amount of TF binding promoter DNA before and after treatment.

Knockdown methods

The cells were transfected using Lipofectamine 2000 (Invitrogen) following the manufacturer's protocol. In brief, the cells were trypsinized and resuspended at a concentration of 2×10^5 cells/mL. For transfection, 2×10^6 cells were plated in the dish. One microgram of DNA was mixed with 50 μL Opti-MEM (Invitrogen) and 3 μL of transfection reagent. After incubated for 20 min, another 50 μL of medium was added. After that, the mixture was dripped into the cells. The ratio of 1 μg of DNA to 3 μL of transfection reagent was maintained for all transfections. Then, the media containing Lipofectamine was replaced the following day. Antibiotics were omitted in the transfection reagents. The small hairpin (sh) DNA were purchased from the National Core Facility at the Institute of Molecular Biology, Genomic Research Center, Academic Sinica, Taiwan. The sh clones TRCN0000274208 and TRCN0000274153 were used to knockdown Sp1 gene and TRCN0000003755 and TRCN0000003756 were used to knock down p53. After transfection, five μg/ml of puromycin was added into the medium for selection. After at least six times of passage, the puromycin-resistant stable cells were generated for further experiments.

Statistics and data analysis

All values were presented as mean ± SEM (standard error of the mean). The figures were depicted by the R or Sigmaplot software. Statistical analysis was performed using the Student *t* test. A *p*-value of less than 0.05 was considered to be statistically significant.

Results

Cordycepin inhibited the growth of MPNST cells without significant synergistic effect when combined with ADA inhibitors

To evaluate the anti-proliferation effect of cordycepin on MPNST cells, the different MPNST (S462TY, ST8814, STS26T, and T265) and normal Schwann cells (HSC) were treated with different concentrations, from 0 up to 1200 μM of cordycepin. As shown in **Figure 1A**, the cell viability showed a dose-dependent decrease, except in HSC and T265. The IC_{50} for S462TY, ST8814, and STS26T cells was 768.6, 300.0, and 268.3 μM. The ST8814 and STS26T cell lines were more sensitive than the S462TY, T265 and normal Schwann cells (HSC) toward cordycepin.

Cordycepin (3'-deoxyadenosine) is the substrate of adenosine deaminase (ADA). Given the anti-proliferative effect of cordycepin on the MPNST cells, we then examined the possible synergistic effect between cordycepin and ADA inhibitors. Two ADA inhibitors, naringin and pentostatin were selected to evaluate the inhibitory effect. In previous study, the IC_{50} of naringin on MG63 and U20S cells at 24 h was found to be around 50 μM and 30 μM, respectively [25]. To inhibit the breast cancer cell lines, MCF-7 and MDA-MG-231, the concentration to inhibit the growth was reported to be between 8.6 and 172 μM [26]. Under the different concentrations between 0 and 100 μM of naringin, there is no significant changes in cell survival among HSC, ST8814, and STS26T cells (Figure S1). As shown in **Figure 1B**, the addition of either 100 or 500 μM of naringin did not enhance the anti-proliferative effect of cordycepin (**Figure 1B** and **1C**). The same findings were shown in another ADA inhibitor, pentostatin (Figure S2).

Cell cycle arrest in G2/M and S phases after treatment of cordycepin

Given the increase of cell death after cordycepin treatment, flow cytometry was employed to explore possible cell cycle arrest induced by cordycepin (**Figure 2A**). The chromosomes of treated cells were stained with propidium iodide to measure the cell population at different cell-cycle stages (P5 = G0/G1, P6 = S, and P7 = G2/M phases). Using ST8814 cells as an example, a significant accumulation of cells in the S phase (P6) after 48 hours of cordycepin treatment (**Figure 2A**) indicated that cordycepin might interfere with the progression of cell cycle.

Most of the cells were in the G0/G1 phase in HSC at baseline, whereas MPNST had more cells in S and G2/M phases (**Figure 2B**). After the treatment with 600 μM of cordycepin for

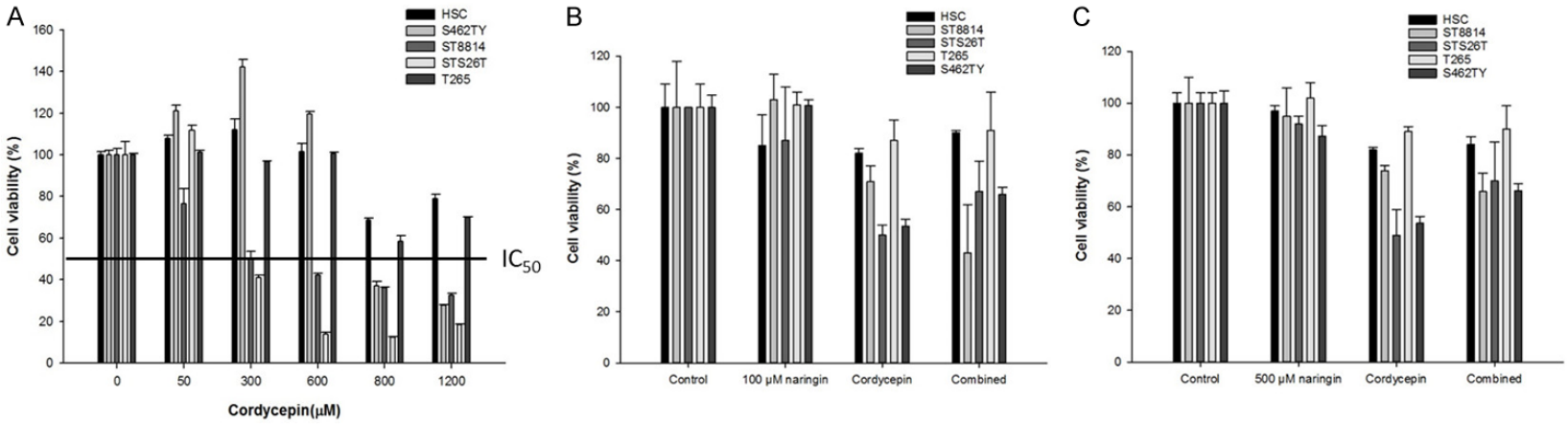

Figure 1. Cell survival in MPNST cell lines after treatment of cordycepin. A. The cell viability (presented in percentage of control) of normal human Schwann cells (HSC) and different MPNST cell lines (S462TY, ST8814, STS26T, and T265) after treated with different concentrations (presented in μM) of cordycepin. B, C. The survival of MPNST cells after the treatment of naringin, cordycepin or the combination of both. Two concentrations of naringin, 100- (1B) and 500-μM (1C) were used to assess any synergistic effect when combined with cordycepin.

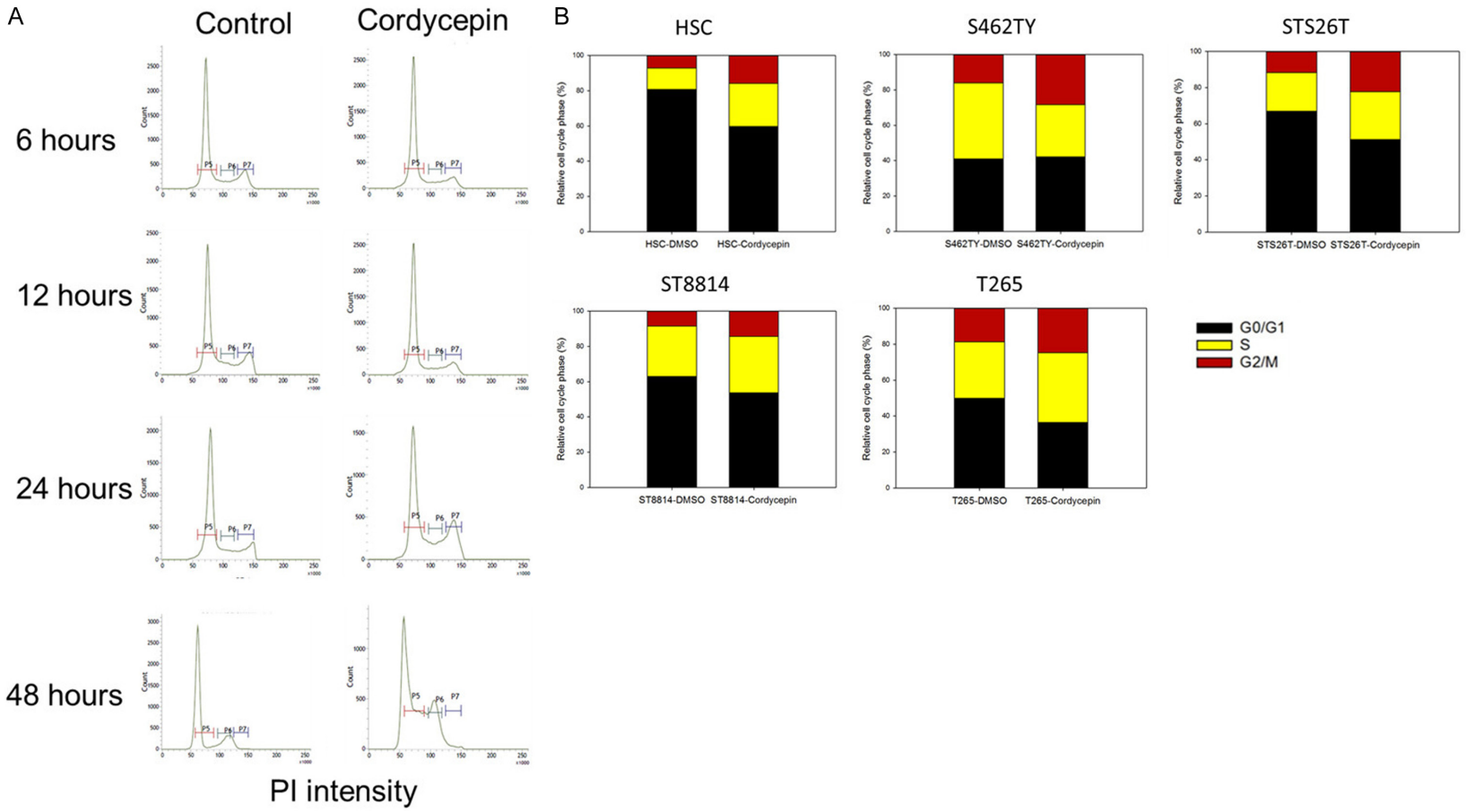

Figure 2. Flow cytometry analysis of MPNST cells after treatment of Cordycepin. A. Flow cytometry analysis of ST8814 cells with/without the treatment of 600 μM of cordycepin. The cell populations at different stages were counted according to the intensity of the propidium iodide (PI), which stained the DNA. The classification of cell stage was dependent on the amount of cellular DNA reflected by the PI intensity. The P5 stage is at G0/G1, P6 is S, and P7 is G2/M phase. Cell populations of ST8814 at P5, P5 and P7 stages did not have a significant change in the control group. However, the populations in P6 and P7 stages increased significantly along with the treatment time. B. The changes of cell population percentages to represent the partition of different phases in cell cycle in HSC and four different MPNST cells after treatment of 600 μM of cordycepin for 24 hrs. The cell population in G2/M and S phases were significantly increased in HSC and MPNST cell lines.

24 hours, the cell populations in S and G2/M phases increased in HSC and all MPNST cell lines (**Figure 2B**). The extent of increase in G2/M phase is significantly larger in the MPNST cell lines than the HSC cells (**Figure 2B**). These findings suggest cordycepin treatment could suppress cell cycle progression through the induction of G2/M and S arrest in HSC and MPNST cells.

Cordycepin treatment inhibited the tumor growth in xenograft mouse model

Since cordycepin suppressed the MPNST cell proliferation *in vitro*, the xenograft mouse model with ST8814 cell inoculation was employed to see if the similar effects could be reproduced *in vivo*. We also evaluated the effect of ADA inhibitor, naringin on the animal model. In every other day, the mice received 67 mg/Kg (about 2 mg/mouse) of cordycepin through intraperitoneal injection (**Figure 3A**). The tumor volume continued to increase in the control group (N = 7) (**Figure 3B**). There was a minor effect on tumor volume in those mice treated with 50 mg/Kg of naringin only (N = 9). However, the size of the tumors decreased significantly after ten days of treatment with cordycepin (N = 7, **Figure 3B**). After treatment of cordycepin for thirty days more than half of the mice were tumor-free. No tumor recurrence was found in those tumor-free mice ten days after stopped the treatment. Likewise, the tumor size decreased significantly in those mice receiving the combined treatment of cordycepin and naringin (N = 11). These findings confirmed that cordycepin could inhibit the MPNST proliferation both *in vitro* and *in vivo*. The treatment of cordycepin in mouse [27] and rat [28] was reported to be safe. There was no decrease of body weight in most of the xenograft mice during the course of treatment (Figure S3). The complete blood cell counts were also unremarkable, but the biochemistry profile showed that the blood level of aspartate aminotransferase increased in those receiving combined treatment (Table S1).

The effect of cordycepin treatment on the levels of cell proliferation-related proteins in MPNST cells

To identify the effect of cordycepin treatment on cell cycle-related proteins, the cells were treated with different concentrations (100, 300, and 600 μM) of cordycepin. The treatment resulted in a dose-dependent decrease in the levels of ERBB2, survivin, $p21^{WARF1}$, and Sp1 (**Figures 4A**, **4B** and S4). There was no change in the level of total ERK protein. However, the immunoblotting showed a decrease of phosphorylated ERK level in the cordycepin-treated MPNST cells, whereas the phosphorylated ERK level increased in the HSC cells. On the other hand, p53 was abundant in the S462TY cells but either absent or nearly absent in the STS26T, ST8814 and T265 cells before cordycepin treatment. After treatment, a slight decrease in p53 was found in the S462TY cells (**Figure 4A**). The phosphorylated AKT protein was increased in HSC, STS26T, T265, and ST8814 cells after treatment (p-AKT in **Figure 4A** and **4B**).

Cordycepin treatment affected the levels of tubulin, actin, and GAPDH

In addition to the effect of proteins related to cell proliferation (**Figure 4**), the changes in tubulin level after cordycepin treatment were also observed. The levels of tubulin-α and -β in MPNST cells after treatment were significantly decreased in a dose-dependent manner (**Figure 5A**). By contrast, the levels of other housekeeping proteins such as actin and glyceraldehyde-3-phosphate dehydrogenase (GAPDH) did not show a significant change after treatment (**Figure 5A**). Since microtubule is composed of both tubulin-α and tubulin-β, the decreased concentration of tubulins may confer the defects of microtubule network. Using immunocytochemistry and confocal microscopy, the shrinkage of the microtubule network was observed (**Figure 5B**). Further assessment of the area of microtubule network showed cordycepin significantly reduced the network in the treated cells, except HSC and T265 cells (**Figure 5C**). These findings indicate that cordycepin treatment could affect the components of microtubule which is involved in chromosome segregation during cell proliferation. Therefore, the decrease of the tubulin level after cordycepin treatment could account for the interference with mitosis and the cell cycle arrest (**Figure 2**).

Epigenetic modification mediates the changes of specific protein levels conferred by cordycepin treatment

As we have shown that the treatment of cordycepin affected the levels of tubulins and some

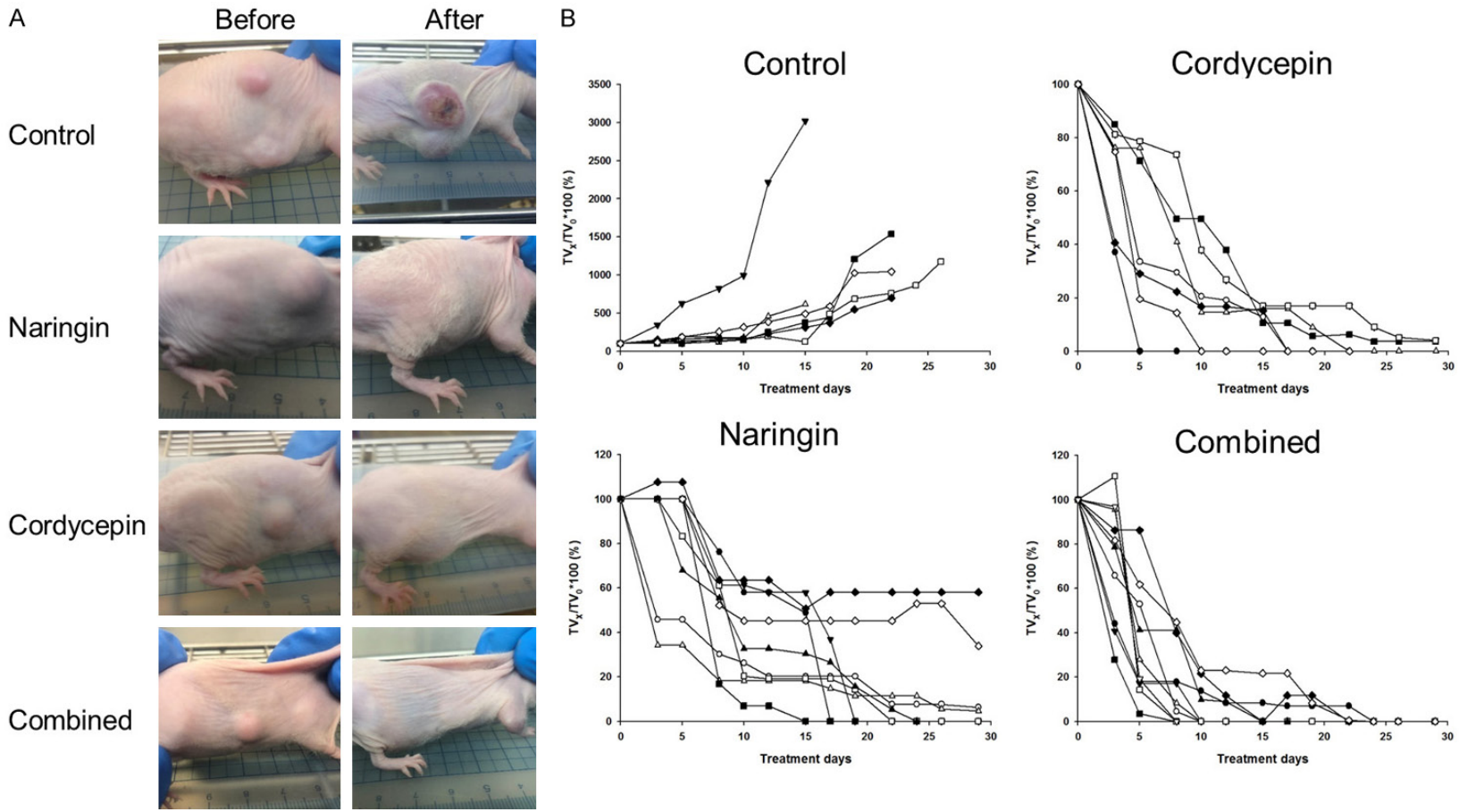

Figure 3. Tumor size of the xenograft mouse model after treatment of cordycepin, naringin or the combination of both. A. The nude mice bearing xenograft tumor were subjected to be assessed of the tumor size to evaluate the effect of cordycepin. There are four groups of xenograft mice. The mice received the total volume of 100 μl of PEG (Control group, N = 7), 67 mg/kg of cordycepin (Cordycepin group, N = 7), 50 mg/kg of naringin (Naringin group, N = 9), and the combination of cordycepin and naringin (Combined group, N = 11). The medications were injected intraperitoneally in every other day. B. The tumor size was represented by the percentage of the original tumor volume (mm^3), which was calculated as, maximum length (mm) × (perpendicular width $(mm)^2$)/2. The size of tumor was recorded during the treatment course, up to 30 days. In addition to evaluating the tumor size, the body weight and activity of animals were also assessed.

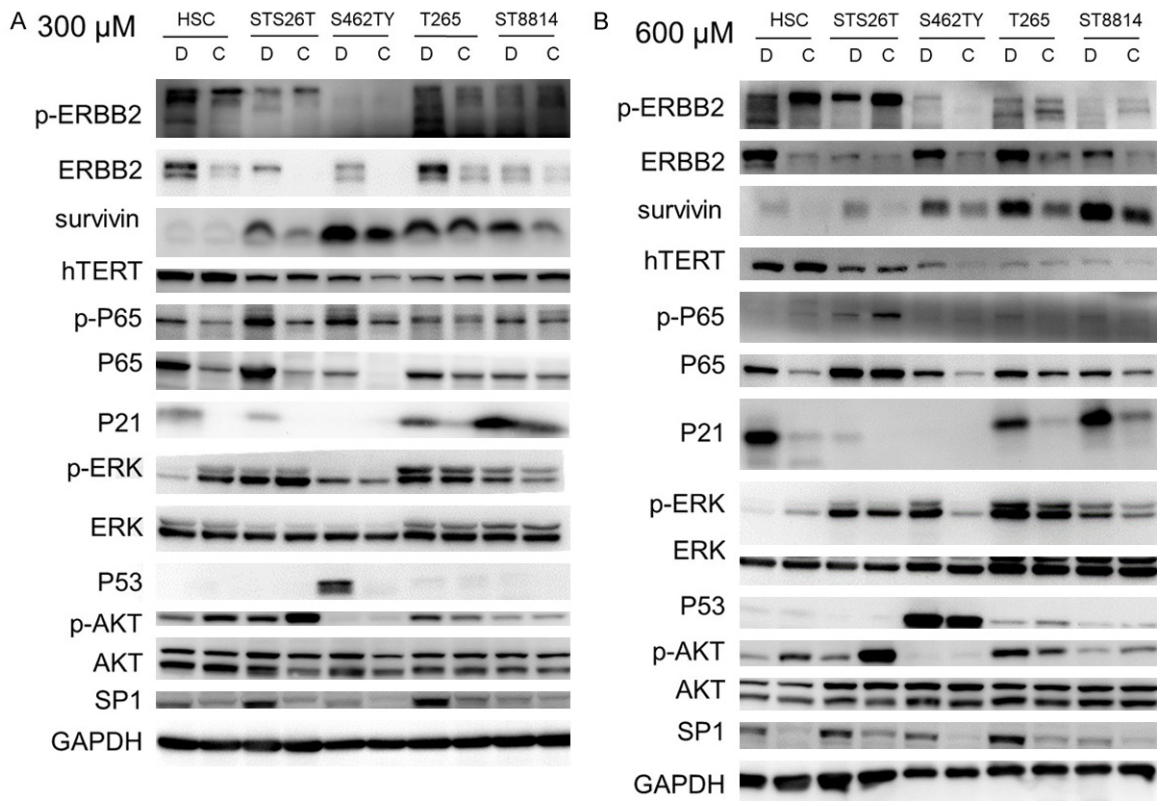

Figure 4. Western blotting for the specific protein levels in MPNST cells after treatment with different concentrations of cordycepin. (A) Immunoblotting of phosphorylated ERBB2 (p-ERBB2), ERBB2, surviving, hTERT, p-p65, p65, $p21^{WARF1}$, p-ERK, ERK, p53, p-AKT, AKT, Sp1 and GAPDH proteins in the normal human Schwann (HSC) and MPNST cells (STS26T, ST8814, T265, and S462TY). The cells were treated with 300 μM of cordycepin. (B) Immunoblotting of the candidate proteins as shown in (A) in HSC and MPNST cells before and after treatment of 600 μM of cordycepin.

cell proliferation-related proteins, whether these changes were caused by the modifications of transcriptional factor (TF) binding sites were investigated. The sequences of the promoter regions were analyzed to identify TF binding sites. As shown in **Figure 6A**, many Sp1 binding sites (GGGCGG) were found on the promoter regions of the *SP1* gene, suggesting a possible positive feedback regulation for the transcription of *SP1*. In addition, a few binding sites for p53 protein (RCWWGY) were also found in the Sp1 promoter region. Both Sp1 and p53 binding sites were observed in *TUBA1A* and *TUBA1B* promoter regions (**Figure 6A**). In the promoter region of the *ACTB* gene, only Sp1 binding sites could be found, whereas only one p53 binding site for the *GAPDH* gene (**Figure 6A**).

We further hypothesized that epigenetic modifications might account for the decrease in tubulin and Sp1 levels after cordycepin treatment. Using chromatin immunoprecipitation (ChIP) with anti-Sp1 antibody, the specific promoter regions that interact with Sp1 protein were pulled-down and quantified. The results showed decreased levels of the *SP1* gene promoter region that bound with Sp1 protein in HSC, ST8814 and STS26T cells, but slightly increased in the S462TY cells (**Figure 6B**). In addition, the levels of Sp1 interacting promoter region for the *TUBA1B* gene was also decreased in HSC, ST8814, and STS26T cells but increased in S462TY cells (**Figure 6B**). These findings suggest cordycepin treatment may decrease the availability of Sp1 protein binding site on the promoter regions of *SP1* and *TUBA1B* genes, leading to the decrease of Sp1 and tubulin protein levels in the HSC, ST8814, and STS26T cells.

The length of the poly(A) tail contributes to the stability and translocation of mRNAs. As mentioned, cordycepin could hamper the normal

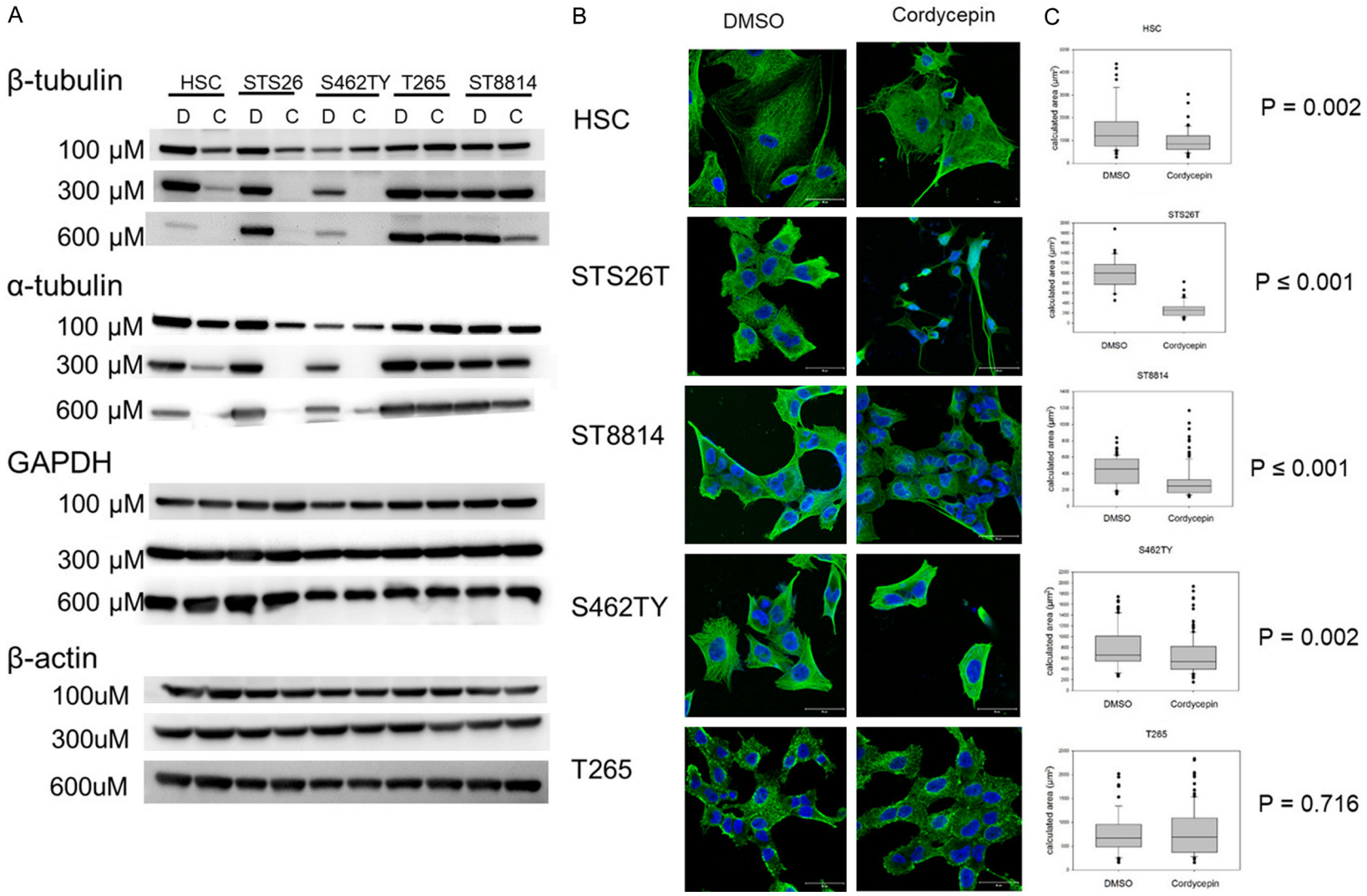

Figure 5. Altered levels of tubulin and the defects of microtubule network after cordycepin treatment. (A) Change of α-, β-tubulin, and GAPDH concentrations in MPNST cells after cells been treated with different concentrations (100, 300, and 600 μM) of cordycepin. The level of tubulin decreased in a dose dependent manner. However, there is no change of concentration in GAPDH. (B) Immunocytochemistry to observe the changes of tubulin level after cordycepin treatment. After 24 hours of treatment of DMSO (control group, left panel) or 600 μM of cordycepin (cordycepin group, right panel), cells were fixed and stained with α-tubulin (green) and DAPI (blue) to examine the changes of tubulin expression. Scale bar, 50 μm. Cell types: Human Schwann Cells (HSC), STS26T, ST8814, and S462TY. (C) Changes of area of microtubule network after treatment of cordycepin. The green area from (B) represented the microtubule network in cytosol. Using Image J software, the stained area of each cell before and after treatment can be calculated. The student *t*-test was employed to compare between the two groups and the *p* value was also presented.

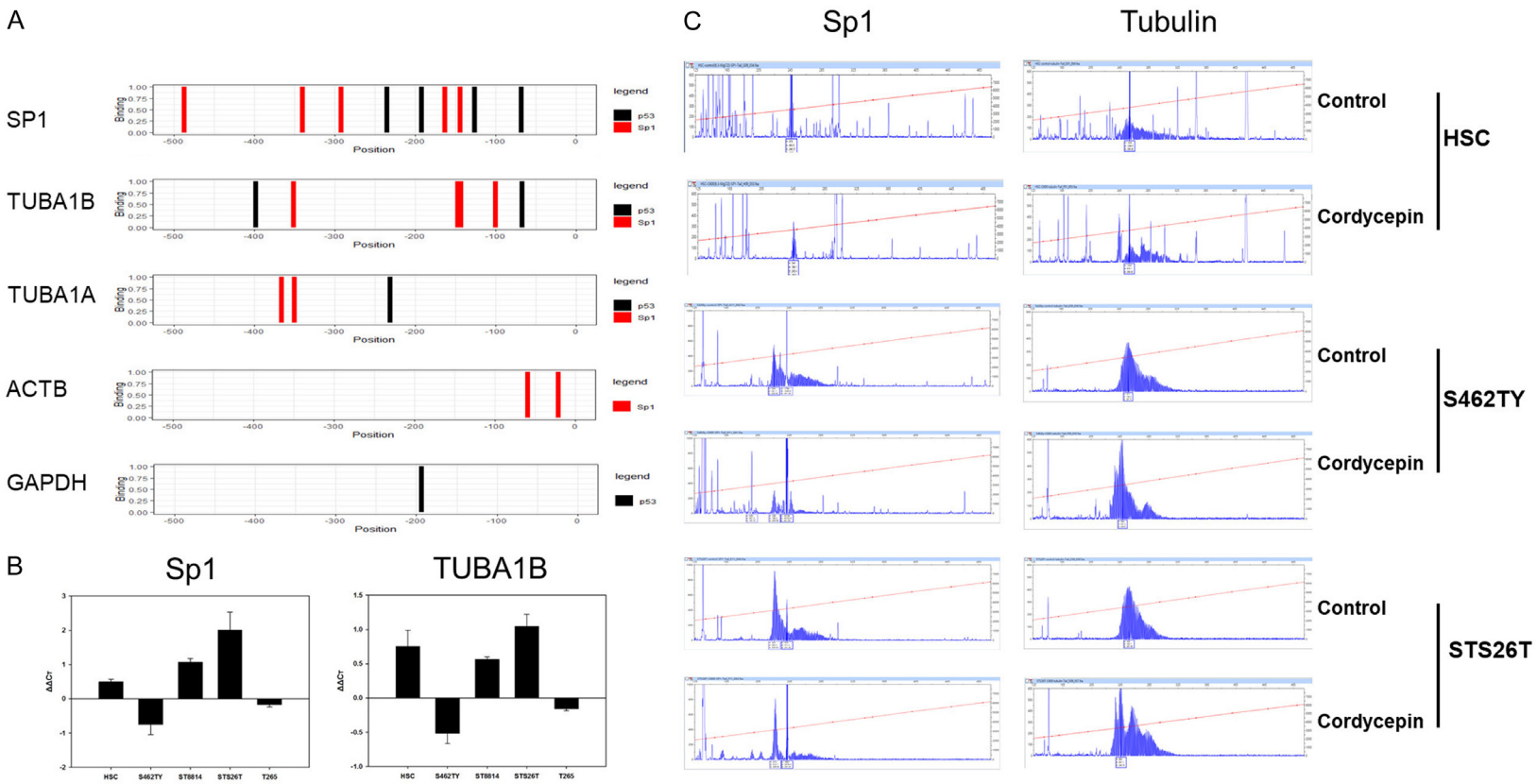

Figure 6. Sp1 transcription factor involves in regulation of tubulin expression after treatment of cordycepin. A. The binding sites of transcriptional factors (Sp1, red; p53, black) in promoter region (0~-500 nucleotide) of the genes, Sp1, TUBA1B, TUBA1A, ACTB and GAPDH genes. B. The value of $\Delta\Delta C_T$ of Sp1 and TUBA1B genes after the treatment of 600 μM of cordycepin in HSC and among different MPNST cell lines, S462TY, ST8814, STS26T and T265. The $\Delta\Delta C_T$ value was obtained from the subtraction of ΔC_T value between before and after treatment. The quantitative PCR was performed using the template DNA which was precipitated (ChIP) by anti-Sp1 antibody. C. The poly(A) tail length of the mRNA of Sp1 and TUBA1B genes in HSC, S462TY and STS26T cells was measured and compared before and after treatment of 600 μM of cordycepin. The cluster of peaks, like shark teeth represents the poly(A) tail which was from the PCR product to amply the 3'end and poly(A) of the candidate gene. The size of poly(A) tail length and the semi-quantitation of the PCR product were assessed using peak scanner software.

polyadenylation during the maturation of mRNA. Therefore, we evaluated whether the treatment of cordycepin might affect the poly(A) tail lengths. As shown in **Figure 6C**, the amount of long poly(A) tail of *SP1* mRNA decreased in S462TY and STS26T cells, but not in HSC after cordycepin treatment. Furthermore, the assay also showed a decrease of *TUBA1B* poly(A) tail length in S462TY and STS26T cells after treatment, but no significant change in HSC cells (**Figure 6C**). These findings suggest the cordycepin treatment can reduce the poly(A) tail length of both *SP1* and *TUBA1B* mRNAs, which also contribute to the suppression of the Sp1 and tubulin protein levels.

The Sp1 protein levels in xenograft tumor tissues before and after cordycepin treatment and in human tumors

Given that the reduced levels of tubulins after cordycepin treatment might be caused by the reduction of the transcription factor Sp1, as shown in our *in vitro* study, immunoblotting using the tumor xenograft (ST8814 cells) was employed to evaluate the Sp1 protein level with or without treatment. The level of Sp1 protein was abundant in the untreated xenograft tumor tissue (PEG group, **Figure 7A**), and decreased significantly after 600 μM of cordycepin treatment (cordycepin group, **Figure 7A**). The calculated mean gray value (integrated density/area) of the tumor slices from PEG treated mice was 57.27 ± 12.80, which is significant larger than that of cordycepin treated mice (46.16 ± 10.00, P = 0.001187, **Figure 7B**).

Moreover, we also observed that the Sp1 protein level was significantly higher in MPNST than in the benign neurofibroma or the adjacent normal tissue from human patients (**Figure 7C**). These findings suggest the overexpression of the transcription factor Sp1 is a common phenomenon in the MPNST. Therefore, cordycepin might have therapeutic implications through reducing the Sp1 level in MPNST.

Transcription factor Sp1 was associated with p53 to control the expression levels of Sp1 and tubulin

The decrease of the Sp1 protein level after cordycepin treatment might contribute to the reduction of tubulins which could presumably lead to the disintegration of the microtubule network and cell cycle arrest (**Figure 4A** and **4B**). We therefore examined whether the treatment of Sp1 inhibitor mithramycin A could induce similar effects on the cells that cordycepin conferred. As shown in **Figure 8A**, the treatment with different concentrations of mithramycin A induced MPNST cell death, most prominently in the STS26T cells. These findings suggest the involvement of Sp1 protein in apoptosis induced by cordycepin. The administration of Sp1 protein did not rescue the cells (**Figure 8B**).

Prior co-immunoprecipitation studies have suggested the association of Sp1 with the p53 proteins [29]. Thus, we hypothesized that the cordycepin-conferred suppression of tubulins might be mediated by Sp1/p53 protein complex instead of Sp1 alone. Since the p53 protein levels are inherently low in STS26T and ST8814 cells, the S462TY cells were used in the study. The left panel of **Figure 8C** showed that the level of Sp1 protein was decreased in the S462TY cells transfected with small-hairpin (sh) Sp1 clone, with the p53 level unperturbed. However, there was a significant reduction of both Sp1 and p53 levels in cells transfected with sh-p53 clones. Furthermore, the tubulin-α and -β levels were reduced in the cells with sh-p53 clone, but not those with sh-Sp1 clone. The S462TY cells with both Sp1 and p53 knockdown were significantly more sensitive to cordycepin treatment than those transfected with scramble clones (right panel of **Figure 8B**). These findings suggest the effects of cordycepin on MPNST cells may depend on the p53/Sp1 protein complex and p53 might govern the integrity of this complex.

Consistent with this, using pifithrin-α (PFT-α) hydrobromide to suppress the level of p53 protein in HSC and S462TY cells made them more vulnerable with a significant decrease of cell survival after the cordycepin treatment (**Figure 8D**). These findings were in line with what we had observed in p53 knockdown cells. Finally, to further validate the hypothesis, we administered different concentrations of recombinant p53 proteins into STS26T and ST8814 cells to see any rescue effect. The addition of p53 protein did significantly rescue both cell lines from the cordycepin treatment (**Figure 8E**). The fact that p53 protein was nearly absent in STS26T

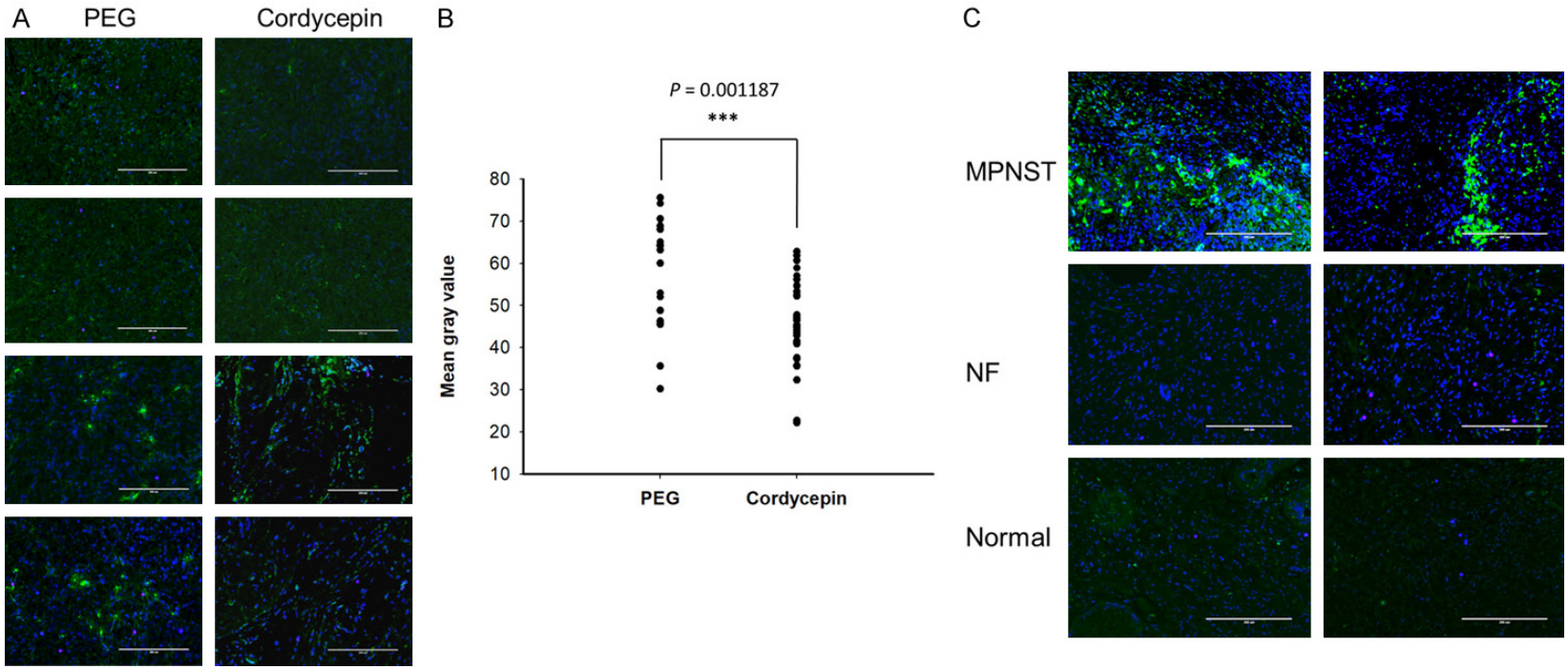

Figure 7. The Sp1 level in tissues from xenograft mouse model after cordycepin treatment (A, B), and from the human patient tissues (C). (A) The level of Sp1 protein in the xenograft tumor tissues from the poly-ethylene glycol (PEG) and cordycepin treated mice. The immunoblotting with anti-Sp1 antibody (green) and DAPI (blue) was observed by the fluorescence microscopy. (B) Mean gray value of the stained tissue slices from the xenograft tumor shown in (A). To analyze the immunohistochemistry staining density of the tissue slice, a semi-quantitation method to measure the mean gray value, defined as integrated density divided by area were used. The values calculated from the tissue slices of PEG treated (N = 18) and cordycepin treated mice (N = 36) were presented. The student *t*-test was employed to compare between the two groups. The mean gray value was significantly decreased in the xenograft tumor from cordycepin treated mice ($P = 0.001187$). (C) The level of Sp1 protein in the MPNST, benign neurofibroma and normal human tissues. Immunostaining of Sp1 protein (green) and DAPI (blue) was observed by the confocal microscopy.

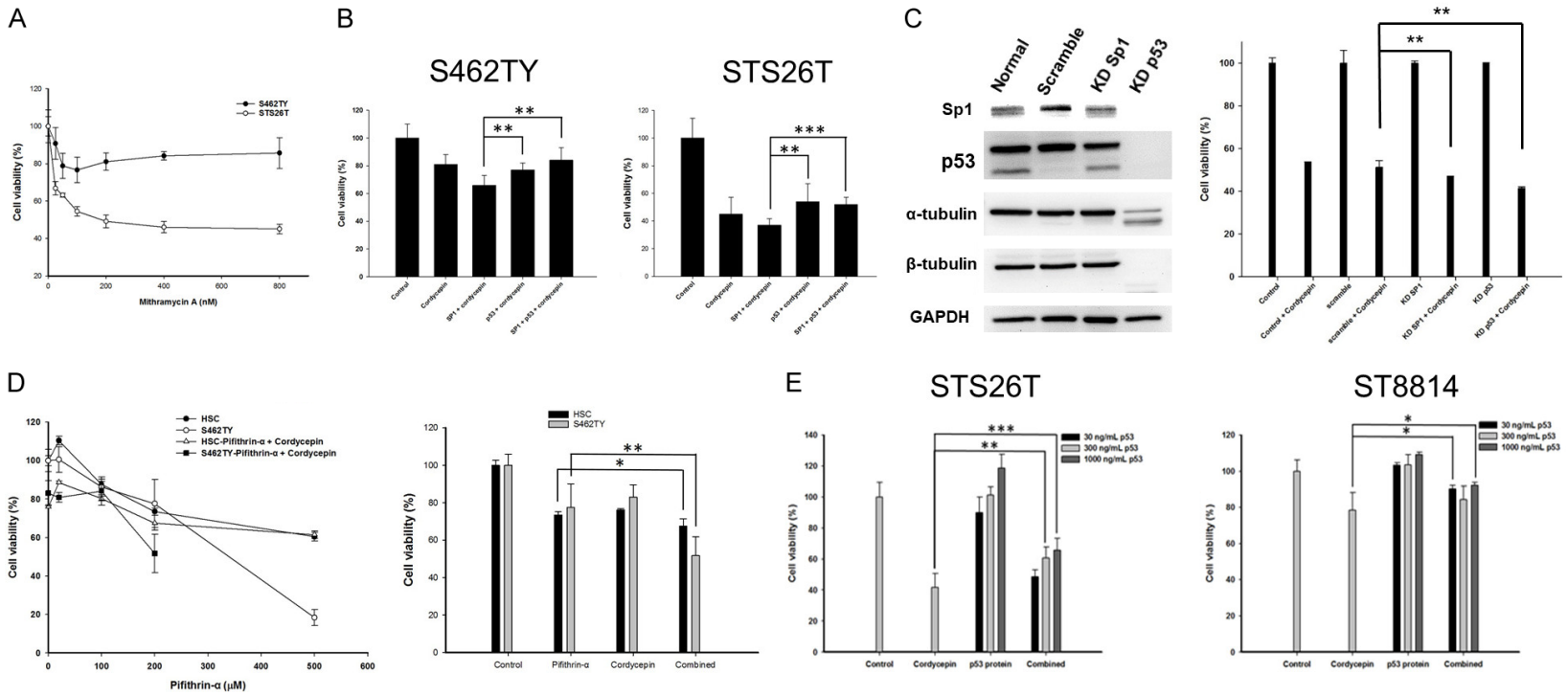

Figure 8. Sp1 associated with p53 proteins increase the survival of MPNST cells after treatment of cordycepin. A. Cell survival after the treatment of different concentrations of mithramycin A. The S462TY and STS26T cells were subjected to MTT assay after the treatment of 0, 25, 50, 100, 200, 400, and 800 μM of mithramycin A. B. Cell viability of S462TY and STS26T cells after the treatment of cordycepin and the combined treatment of cordycepin, Sp1 and p53 proteins. The cells were incubated with 600 μM cordycepin for 24 hours before MTT assay. Three more groups with combined treatment were also subjected to cell survival assay. In addition to cordycepin, one group combined with 500 ng/mL of Sp1 recombinant protein, one with 1000 ng/mL of p53 protein and one with both proteins. The student *t*-test was employed to compare between the two groups (*, $P < 0.05$, **, $P < 0.01$). C. Knockdown the expression of Sp1 and p53 mRNA transcripts of S462TY cells and the cell survival assay in these cells after treatment of 600 μM of cordycepin. The student *t*-test was employed to compare between the two groups (**, $P < 0.01$). D. Cell survival of human Schwann cell (HSC) and S462TY cells after the treatment of pifithrin-α. Left panel, cell viability of HSC and S462TY cells after the combined treatment of cordycepin and different concentrations (20, 50, 100, 200 and 500 μM) of pifithrin-α. Right panel, cell viability of HSC and S462TY cells after the treatment of 200 μM of pifithrin-α, 600 μM of cordycepin or both combination. The student *t*-test was employed to compare between the two groups (*, $P < 0.05$, **, $P < 0.01$). E. Cell survival of STS26T and SY8814 cells after the treatment of 600 μM of cordycepin along with different concentrations (30, 300 and 1000 ng/mL) of recombinant human p53 protein. The MTT assay has been performed after incubation of 24 hours. The student *t*-test was employed to compare between the two groups (*, $P < 0.05$, **, $P < 0.01$, ***, $P < 0.001$).

and ST8814 cells could explain why these cells were more vulnerable to cordycepin treatment than S462TY cells that have a higher p53 level.

Discussion

MPNST is intractable and no armamentarium has been proved to be effective in treating the disease. We demonstrated the suppression of the MPNST cell growth by cordycepin, an adenosine analog, both *in vitro* and *in vivo*. The addition of adenosine metabolizing enzyme, ADA (adenosine deaminase) inhibitors, either pentostatin or naringin, did not confer a synergistic effect *in vitro*. The cordycepin treatment resulted in G2/M and S phases cell cycle arrest in MPNST and HSC cells. The *in vivo* study on the xenograft mice showed cordycepin was efficient to inhibit the cell proliferation or could even eradicate the grafted MPNST cells. Immunoblotting showed a significant reduction of tubulin, but not actin or GAPDH in the MPNST cells after cordycepin treatment. Reduction of tubulin level could disrupt the integrity of the microtubule network. The decrease of tubulin proteins after cordycepin treatment was probably the result of suppressing Sp1, a transcriptional factor (TF) binding to the promoter regions of the tubulin genes. In addition, the decrease of poly(A) tail length of the *SP1* and *TUBA1B* mRNAs after cordycepin treatment could destabilize the transcripts which might also contribute to the reduction of protein levels. The treatment of mithramycin A, an inhibitor for Sp1 activity, resulted in cell apoptosis; however, the addition of Sp1 recombinant protein did not rescue the effect of cordycepin. The levels of both Sp1 and p53 proteins and the tubulins were reduced significantly in the S462TY cells with p53 knockdown, but not in the cells with Sp1 knockdown. Moreover, p53 knockdown cells showed a higher susceptibility toward cordycepin treatment than the cells transfected with a scrambled sequence. In line with the knockdown experiment, the administration of pifithrin-α, a p53 protein inhibitor, also made the cells more sensitive to cordycepin. Adding p53 recombinant protein reverted the cells from the inhibitory effect of cordycepin.

Adenosine deaminase (ADA) hydrolyzes the adenosine and its derivatives, such as cordycepin [30]. The half-life of cordycepin is short *in vivo* in both rat (t1/2 = 1.6 min) [31] and human [32]. Thus either structure modifications or high therapeutic dosage is required to further develop cordycepin for clinical usage. The inhibition of ADA may impede the degradation of cordycepin, which may consequently enhance the anticancer effect of cordycepin. We applied the combination of ADA inhibitors, either pentostatin and naringin, with cordycepin to the MPNST cells, but no significant synergistic effect was found *in vitro*. Nevertheless, the treatment of naringin alone in xenograft mice showed a decrease in tumor size. Moreover, the xenograft mice became tumor-free after the combined treatment of naringin and cordycepin. These findings indicate that the inhibition of ADA activity is manifested *in vivo*, but somehow not significant *in vitro*. It has been reported that there is differential anticancer effect of the ADA inhibitors such as EHNA and pentostatin [33]. In addition to chemotherapeutic effect, naringin involves in multiple biological functions such as anti-free radical effect, anti-inflammation, potentiate the immune reaction etc. The discrepancy between the *in vivo* and *in vitro* effects of naringin might be due to the immune reaction of the animal model as those reported in the preclinical studies [26].

The length of poly(A) tail at the 3'-end of mRNA has recently been linked to cell apoptosis [34]. The two-step reaction, endonucleolytic cleavage of pre-mRNA followed by the addition of a poly(A) tail at 3'end, determines the stability and the translational ability of mRNAs [35, 36]. Polyadenylation polymerase (PAP) is one of the most studied proteins in the polyadenylation protein complex. The pharmacological effect of cordycepin has been proposed to be attributed to its inhibitory effect on poly(A) synthesis, which interferes with the maturation and processing of the nascent mRNA [37]. Polyadenylation inhibitors including cordycepin can decrease cell proliferation and increase apoptosis in cancer cells [20, 34]. The proper regulation on the length of poly(A) tail is crucial for maintaining the biological function of mRNAs in cells. Nevertheless, poly(A) tail length control and development go hand in hand. Whether the tails need to be shorter or longer depends on the nascent transcripts [38]. Genes involved in apoptosis, such as bcl2 and p53, were regulated via mRNA stabilization/destabilization [39, 40]. For example, the p53/p-AKT was found to

be involved in the process of stabilizing the mRNA in cancer cells via controlling the activity of PAP. These findings suggested the post-transcriptional regulations are dynamically regulated in cancers. Our study demonstrated that cordycepin induced apoptosis in MPNST cells and reduced the length of poly(A) tail in both Sp1 and TUBA1B genes, which might contribute to the decrease of Sp1 and TUBA1B protein levels.

The α- and β-tubulin are the basic structural unit of the microtubule. These units stack on top of one another to form strips which align with other strips and form a hollow tube, *i.e.*, the microtubule. Microtubules grow by continually adding more tubulin from their free ends. If they stop growing, microtubules would rapidly fall apart or depolymerize to release tubulin for recycling. The dynamic instability due to the stochastic switching between growing and shrinking is essential for microtubule function. The switching was found to be driven by GTP hydrolysis in the lattice of microtubules. Recently, the microtubules were targeted by a number of anticancer agents. For example, taxol was found to be able to insert into the tubulin protein and prevent microtubule depolymerization [41]. In addition to the defects in mitosis, the shrinkage and disruption of microtubules also significantly suppressed endothelial VEGFR2 mRNA expression and accumulation. The repression was found to be conveyed by two consensus Sp1-binding sites at the promoter region of the VEGFR2 gene. Further electrophoretic mobility-shift assay analysis revealed that in cells with microtubule disassembly, the constitutive Sp1-dependent DNA binding was decreased [42].

Recently, a novel histone deacetylases (HDAC) inhibitor, WMJ-8-B, was shown to reduce the expression of survivin in MDA-MB-231 breast cancer cells and cause the G2/M cell cycle arrest. WMJ-8-B increased the transcription factor Sp1 binding to the p21 promoter region. Furthermore, it also induced α-tubulin acetylation and disrupted microtubule assembly [43]. Camptothecin (CPT), which targets topoisomerase I, was found to be effective to induce the mitotic cell arrest. Upon exposure to CPT, c-Jun N-terminal kinase (JNK) acts upstream of Sp1 with further up-regulates p21-mediated mitotic arrest. Their results suggest that CPT, the topoisomerase I-mediated tubulin-targeting drugs can lead to mitotic arrest by upregulating Mad2 through the JNK-mediated Sp1 pathway and autophagy formation from tubulin polymerization [44]. Although both compounds are tubulin-targeting drugs able to induce the microtubule disassembly, the binding of Sp1 leads to the increase level of $p21^{WARF}$ which is divergent to our findings. Cordycepin treatment suppressed the expression of Sp1 and $p21^{WARF}$ in MPNST cells.

Our study demonstrated the change of tubulin level after cordycepin treatment. The p53 pathways associated with MAPK and PI3K/AKT signaling pathways play an important role in cordycepin-induced apoptosis, which has also been reported in other studies [15, 45-47]. In the human uterine cervical cancer cell line, ME180, cordycepin extended the radiation-induced G2/M arrest and increased the p53 level [48]. A recent study explored the molecular landscape of glioma from patients with neurofibromatosis type 1 [49]. The comparison of the genetic alterations between the low-grade and high-grade gliomas demonstrated significant differences in PI3 kinase, transcription/chromatin regulation, RNA splicing, MAPK and cilium/centrosome pathways. Genetic variances leading to the dysfunction of molecular pathways of PI3K-AKT and transcription/chromatin regulation occurred more frequently in high-grade glioma.

Chua *et al*. showed that p53 together with Sp1 bound to the ZID elements at the promoter region of BZLF1 gene of the EB virus [29]. The immunoprecipitation results showed the co-precipitation of p53 and Sp1, suggesting these two TFs were associated together. The study of MnSOD expression regulation also found the co-immunoprecipitation of Sp1 and p53 [50]. The interplay between Sp1 and p53 is complicated and may be cell-type specific. Our study demonstrated that the Sp1 expression was concurrently silenced in the S462TY cells when p53 was knocked down by shRNA. The levels of both α- and β-tubulins decreased as well in the p53-knocked-down cells. However, those cells transfected with Sp1 shRNA clones did not show a significant reduction of the p53 and tubulin levels. In contrast to the cooperation in mediating transcription regulation, studies showed the competition between Sp1 and p53 in binding to specific promoters and that they might function in opposite directions [51]. For

example, Sp1 was found to be required to activate T-antigen expression, whereas p53 was found to repress its transcription [52]. The p53/Sp1-associated protein complex can enhance the NF-κB mediated MnSOD expression. On the contrary, this complex suppressed both the constitutive and phorbol ester-stimulated expression of MnSOD gene which harbors a strong protection from cell death [50]. Thus, the interplay between Sp1 and p53 demonstrates an intricate relationship between the positive and negative regulations on the expression of specific genes.

Inhibition of Sp1 protein by mithramycin A can induce cell death, especially in STS26T cells. The addition of Sp1 protein cannot totally rescue the cells from apoptosis caused by cordycepin (**Figure 8B**). Knocking down the Sp1 or p53 made the S462TY cells more vulnerable to cordycepin (**Figure 8C**). Moreover, the administration of p53 significantly salvaged the STS-26T and ST8814 cells which were inherently p53-deficient. These findings suggest that both p53 and Sp1 contribute to the regulation of Sp1 and tubulin protein levels.

In summary, we showed that cordycepin inhibits the proliferation of MPNST cells both *in vitro* and *in vivo*. The treatment causes the decrease expression of tubulin levels which leads to a defect of microtubule network and chromosome mis-segregation. The transcription factor, Sp1 and p53 binds to the promoter region of *SP1* gene which further regulates the transcription of *SP1*, *TUBA1B* and *TUBA1A* genes. Cordycepin treatment markedly reduced the expression of Sp1 protein. Moreover, cordycepin can reduce the *SP1*, *TUBA1B* and *TUBA1A* mRNA poly(A) tail length and destabilized the mRNAs. Thus, these effects may contribute to the down-regulation of tubulin proteins. The administration of Sp1 protein cannot rescue the cell death after treatment, but the addition of p53 or the combination of Sp1 and p53 can ameliorate the cordycepin effects. The S462TY cells have high level of p53 protein. When knocking down the p53 with shRNA, both p53 and Sp1 protein levels in S462TY cells were decreased, which render the cells more sensitive to cordycepin. These findings suggest p53 and Sp1 proteins interact as a complex and cordycepin induces MPNST cell death may be through the p53/Sp1/tubulin pathway.

Acknowledgements

We would like to thank the technique and facility support from the second and the third common laboratory, National Taiwan University Hospital, Taipei, Taiwan. This research was funded by Ministry of Science and Technology, grant number MOST 108-2314-B-002-081 and MOST 109-2314-B-002-121-MY3, and also by National Taiwan University Hospital, grant number NTUH 109-004528.

Disclosure of conflict of interest

None.

Address correspondence to: Dr. Ming-Jen Lee, Department of Neurology, National Taiwan University Hospital, National Taiwan University College of Medicine, Taipei, Taiwan. Tel: +886-2-23123456 Ext. 65336; E-mail: mjlee@ntu.edu.tw; Dr. Kai Wang, Institute for Systems Biology, Seattle, Washington, USA. Tel: +1-206-732-1336; E-mail: kai.wang@isbscience.org

References

[1] Friedman JM and Birch PH. Type 1 neurofibromatosis: a descriptive analysis of the disorder in 1,728 patients. Am J Med Genet 1997; 70: 138-143.

[2] Lee MJ and Stephenson DA. Recent developments in neurofibromatosis type 1. Curr Opin Neurol 2007; 20: 135-141.

[3] Darrigo LG Jr, Geller M, Bonalumi Filho A and Azulay DR. Prevalence of plexiform neurofibroma in children and adolescents with type I neurofibromatosis. J Pediatr (Rio J) 2007; 83: 571-573.

[4] Hirbe AC and Gutmann DH. Neurofibromatosis type 1: a multidisciplinary approach to care. Lancet Neurol 2014; 13: 834-843.

[5] Korf BR. Plexiform neurofibromas. Am J Med Genet 1999; 89: 31-37.

[6] Lowe SW, Cepero E and Evan G. Intrinsic tumour suppression. Nature 2004; 432: 307-315.

[7] Bai J, Li Y and Zhang G. Cell cycle regulation and anticancer drug discovery. Cancer Biol Med 2017; 14: 348-362.

[8] Evan GI and Vousden KH. Proliferation, cell cycle and apoptosis in cancer. Nature 2001; 411: 342-348.

[9] Cunningham KG, Manson W, Spring FS and Hutchinson SA. Cordycepin, a metabolic product isolated from cultures of Cordyceps militaris (Linn.) Link. Nature 1950; 166: 949.

[10] Nakamura K, Yoshikawa N, Yamaguchi Y, Kagota S, Shinozuka K and Kunitomo M. Antitumor effect of cordycepin (3'-deoxyadenosine) on mouse melanoma and lung carcinoma cells involves adenosine A3 receptor stimulation. Anticancer Res 2006; 26: 43-47.
[11] Koc Y, Urbano AG, Sweeney EB and McCaffrey R. Induction of apoptosis by cordycepin in ADA-inhibited TdT-positive leukemia cells. Leukemia 1996; 10: 1019-1024.
[12] Panicali DL and Nair CN. Effect of cordycepin triphosphate on in vitro RNA synthesis by picornavirus polymerase complexes. J Virol 1978; 25: 124-128.
[13] Sugar AM and McCaffrey RP. Antifungal activity of 3'-deoxyadenosine (cordycepin). Antimicrob Agents Chemother 1998; 42: 1424-1427.
[14] Cho HJ, Cho JY, Rhee MH and Park HJ. Cordycepin (3'-deoxyadenosine) inhibits human platelet aggregation in a cyclic AMP- and cyclic GMP-dependent manner. Eur J Pharmacol 2007; 558: 43-51.
[15] Liao Y, Ling J, Zhang G, Liu F, Tao S, Han Z, Chen S, Chen Z and Le H. Cordycepin induces cell cycle arrest and apoptosis by inducing DNA damage and up-regulation of p53 in Leukemia cells. Cell Cycle 2015; 14: 761-771.
[16] Takahashi S, Tamai M, Nakajima S, Kato H, Johno H, Nakamura T and Kitamura M. Blockade of adipocyte differentiation by cordycepin. Br J Pharmacol 2012; 167: 561-575.
[17] Won KJ, Lee SC, Lee CK, Lee HM, Lee SH, Fang Z, Choi OB, Jin M, Kim J, Park T, Choi WS, Kim SK and Kim B. Cordycepin attenuates neointimal formation by inhibiting reactive oxygen species-mediated responses in vascular smooth muscle cells in rats. J Pharmacol Sci 2009; 109: 403-412.
[18] Muller WE, Seibert G, Beyer R, Breter HJ, Maidhof A and Zahn RK. Effect of cordycepin on nucleic acid metabolism in L5178Y cells and on nucleic acid-synthesizing enzyme systems. Cancer Res 1977; 37: 3824-3833.
[19] Penman S, Rosbash M and Penman M. Messenger and heterogeneous nuclear RNA in HeLa cells: differential inhibition by cordycepin. Proc Natl Acad Sci U S A 1970; 67: 1878-1885.
[20] Imesch P, Hornung R, Fink D and Fedier A. Cordycepin (3'-deoxyadenosine), an inhibitor of mRNA polyadenylation, suppresses proliferation and activates apoptosis in human epithelial endometriotic cells in vitro. Gynecol Obstet Invest 2011; 72: 43-49.
[21] Camargo CA, Gomes-Marcondes MC, Wutzki NC and Aoyama H. Naringin inhibits tumor growth and reduces interleukin-6 and tumor necrosis factor alpha levels in rats with Walker 256 carcinosarcoma. Anticancer Res 2012; 32: 129-133.
[22] Cheson BD, Vena DA, Barrett J and Freidlin B. Second malignancies as a consequence of nucleoside analog therapy for chronic lymphoid leukemias. J Clin Oncol 1999; 17: 2454-2460.
[23] Miller SJ, Rangwala F, Williams J, Ackerman P, Kong S, Jegga AG, Kaiser S, Aronow BJ, Frahm S, Kluwe L, Mautner V, Upadhyaya M, Muir D, Wallace M, Hagen J, Quelle DE, Watson MA, Perry A, Gutmann DH and Ratner N. Large-scale molecular comparison of human schwann cells to malignant peripheral nerve sheath tumor cell lines and tissues. Cancer Res 2006; 66: 2584-2591.
[24] Johansson G, Mahller YY, Collins MH, Kim MO, Nobukuni T, Perentesis J, Cripe TP, Lane HA, Kozma SC, Thomas G and Ratner N. Effective in vivo targeting of the mammalian target of rapamycin pathway in malignant peripheral nerve sheath tumors. Mol Cancer Ther 2008; 7: 1237-1245.
[25] Ming H, Chuang Q, Jiashi W, Bin L, Guangbin W and Xianglu J. Naringin targets Zeb1 to suppress osteosarcoma cell proliferation and metastasis. Aging (Albany NY) 2018; 10: 4141-4151.
[26] Bharti S, Rani N, Krishnamurthy B and Arya DS. Preclinical evidence for the pharmacological actions of naringin: a review. Planta Med 2014; 80: 437-451.
[27] Su NW, Wu SH, Chi CW, Liu CJ, Tsai TH and Chen YJ. Metronomic cordycepin therapy prolongs survival of oral cancer-bearing mice and inhibits epithelial-mesenchymal transition. Molecules 2017; 22: 629.
[28] Aramwit P, Porasuphatana S, Srichana T and Nakpheng T. Toxicity evaluation of cordycepin and its delivery system for sustained in vitro anti-lung cancer activity. Nanoscale Res Lett 2015; 10: 152.
[29] Chua HH, Chiu HY, Lin SJ, Weng PL, Lin JH, Wu SW, Tsai SC and Tsai CH. p53 and Sp1 cooperate to regulate the expression of Epstein-Barr viral Zta protein. J Med Virol 2012; 84: 1279-1288.
[30] Cristalli G, Costanzi S, Lambertucci C, Lupidi G, Vittori S, Volpini R and Camaioni E. Adenosine deaminase: functional implications and different classes of inhibitors. Med Res Rev 2001; 21: 105-128.
[31] Tsai YJ, Lin LC and Tsai TH. Pharmacokinetics of adenosine and cordycepin, a bioactive constituent of Cordyceps sinensis in rat. J Agric Food Chem 2010; 58: 4638-4643.
[32] Niramitranon J and Pongprayoon P. Exploring the binding modes of cordycepin to human adenosine deaminase 1 (ADA1) compared to ad-

enosine and 2'-deoxyadenosine. J Mol Model 2020; 26: 29.
[33] Nakajima Y, Kanno T, Nagaya T, Kuribayashi K, Nakano T, Gotoh A and Nishizaki T. Adenosine deaminase inhibitor EHNA exhibits a potent anticancer effect against malignant pleural mesothelioma. Cell Physiol Biochem 2015; 35: 51-60.
[34] Thomadaki H, Scorilas A, Tsiapalis CM and Havredaki M. The role of cordycepin in cancer treatment via induction or inhibition of apoptosis: implication of polyadenylation in a cell type specific manner. Cancer Chemother Pharmacol 2008; 61: 251-265.
[35] Wahle E and Ruegsegger U. 3'-End processing of pre-mRNA in eukaryotes. FEMS Microbiol Rev 1999; 23: 277-295.
[36] Zhao J, Hyman L and Moore C. Formation of mRNA 3' ends in eukaryotes: mechanism, regulation, and interrelationships with other steps in mRNA synthesis. Microbiol Mol Biol Rev 1999; 63: 405-445.
[37] Johns DG and Adamson RH. Enhancement of the biological activity of cordycepin (3'-deoxyadenosine) by the adenosine deaminase inhibitor 2'-deoxycoformycin. Biochem Pharmacol 1976; 25: 1441-1444.
[38] Jalkanen AL, Coleman SJ and Wilusz J. Determinants and implications of mRNA poly(A) tail size--does this protein make my tail look big? Semin Cell Dev Biol 2014; 34: 24-32.
[39] Kim H, You S, Foster LK, Farris J and Foster DN. The rapid destabilization of p53 mRNA in immortal chicken embryo fibroblast cells. Oncogene 2001; 20: 5118-5123.
[40] Schiavone N, Rosini P, Quattrone A, Donnini M, Lapucci A, Citti L, Bevilacqua A, Nicolin A and Capaccioli S. A conserved AU-rich element in the 3' untranslated region of bcl-2 mRNA is endowed with a destabilizing function that is involved in bcl-2 down-regulation during apoptosis. FASEB J 2000; 14: 174-184.
[41] Alushin GM, Lander GC, Kellogg EH, Zhang R, Baker D and Nogales E. High-resolution microtubule structures reveal the structural transitions in alphabeta-tubulin upon GTP hydrolysis. Cell 2014; 157: 1117-1129.
[42] Meissner M, Pinter A, Michailidou D, Hrgovic I, Kaprolat N, Stein M, Holtmeier W, Kaufmann R and Gille J. Microtubule-targeted drugs inhibit VEGF receptor-2 expression by both transcriptional and post-transcriptional mechanisms. J Invest Dermatol 2008; 128: 2084-2091.
[43] Chuang YF, Huang SW, Hsu YF, Yu MC, Ou G, Huang WJ and Hsu MJ. WMJ-8-B, a novel hydroxamate derivative, induces MDA-MB-231 breast cancer cell death via the SHP-1-STAT3-survivin cascade. Br J Pharmacol 2017; 174: 2941-2961.
[44] Dilshara MG, Jayasooriya R, Karunarathne W, Choi YH and Kim GY. Camptothecin induces mitotic arrest through Mad2-Cdc20 complex by activating the JNK-mediated Sp1 pathway. Food Chem Toxicol 2019; 127: 143-155.
[45] Chen Y, Yang SH, Hueng DY, Syu JP, Liao CC and Wu YC. Cordycepin induces apoptosis of C6 glioma cells through the adenosine 2A receptor-p53-caspase-7-PARP pathway. Chem Biol Interact 2014; 216: 17-25.
[46] Lin YT, Liang SM, Wu YJ, Wu YJ, Lu YJ, Jan YJ, Ko BS, Chuang YJ, Shyue SK, Kuo CC and Liou JY. Cordycepin suppresses endothelial cell proliferation, migration, angiogenesis, and tumor growth by regulating focal adhesion kinase and p53. Cancers (Basel) 2019; 11: 168.
[47] Lu Q, Mei W, Luo S and He W. Apoptosis of Bel-7402 human hepatoma cells induced by a ruthenium(II) complex coordinated by cordycepin through the p53 pathway. Mol Med Rep 2015; 11: 4424-4430.
[48] Seong da B, Hong S, Muthusami S, Kim WD, Yu JR and Park WY. Cordycepin increases radiosensitivity in cervical cancer cells by overriding or prolonging radiation-induced G2/M arrest. Eur J Pharmacol 2016; 771: 77-83.
[49] D'Angelo F, Ceccarelli M, Tala, Garofano L, Zhang J, Frattini V, Caruso FP, Lewis G, Alfaro KD, Bauchet L, Berzero G, Cachia D, Cangiano M, Capelle L, de Groot J, DiMeco F, Ducray F, Farah W, Finocchiaro G, Goutagny S, Kamiya-Matsuoka C, Lavarino C, Loiseau H, Lorgis V, Marras CE, McCutcheon I, Nam DH, Ronchi S, Saletti V, Seizeur R, Slopis J, Sunol M, Vandenbos F, Varlet P, Vidaud D, Watts C, Tabar V, Reuss DE, Kim SK, Meyronet D, Mokhtari K, Salvador H, Bhat KP, Eoli M, Sanson M, Lasorella A and Iavarone A. The molecular landscape of glioma in patients with Neurofibromatosis 1. Nat Med 2019; 25: 176-187.
[50] Dhar SK, Xu Y, Chen Y and St Clair DK. Specificity protein 1-dependent p53-mediated suppression of human manganese superoxide dismutase gene expression. J Biol Chem 2006; 281: 21698-21709.
[51] Oppenheim A and Lahav G. The puzzling interplay between p53 and Sp1. Aging (Albany NY) 2017; 9: 1355-1356.
[52] Drayman N, Ben-Nun-Shaul O, Butin-Israeli V, Srivastava R, Rubinstein AM, Mock CS, Elyada E, Ben-Neriah Y, Lahav G and Oppenheim A. p53 elevation in human cells halt SV40 infection by inhibiting T-ag expression. Oncotarget 2016; 7: 52643-52660.

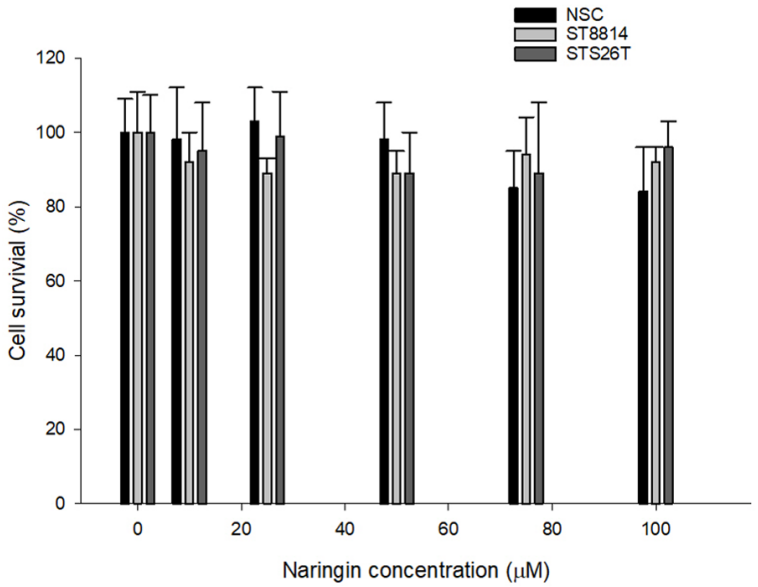

Figure S1. Viability of HSC, ST8814 and STS26T cells after the treatment of different concentrations of naringin. Human Schwann cells (HSC) and MPNST cell lines (ST8814 and STS26T) were treated with naringin. The concentrations of naringin were 0, 10, 25, 50, 75, and 100 μM. After treatment, the cell survival was calculated by MTT assay.

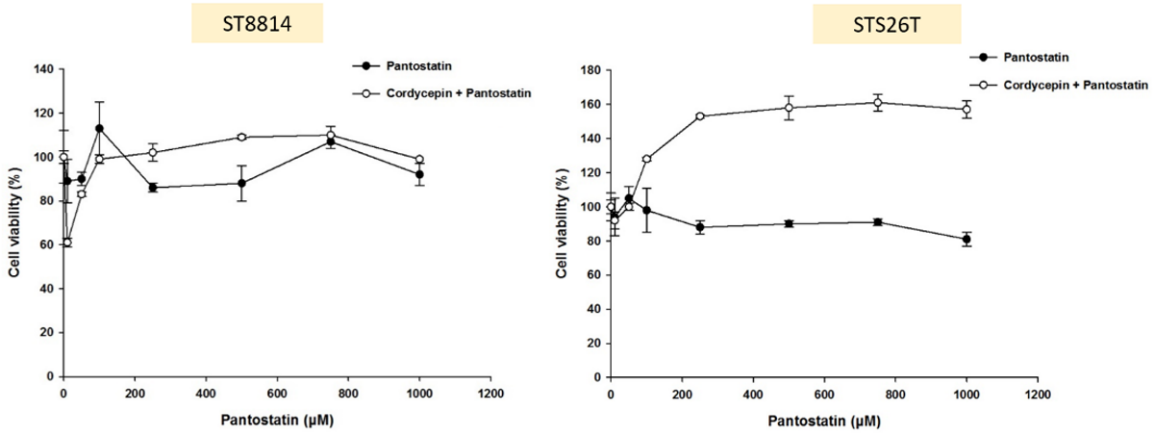

Figure S2. Viability of ST8814 and STS26T cells after the treatment of different concentrations of pantostatin. Two MPNST cell lines (ST8814 and STS26T) were treated by either pentostatin alone or in combination with 600 μM of cordycepin. The concentrations of pentostatin were 0, 100, 250, 500, 750, and 1000 μM. After treatment, the cell survival was calculated by MTT assay.

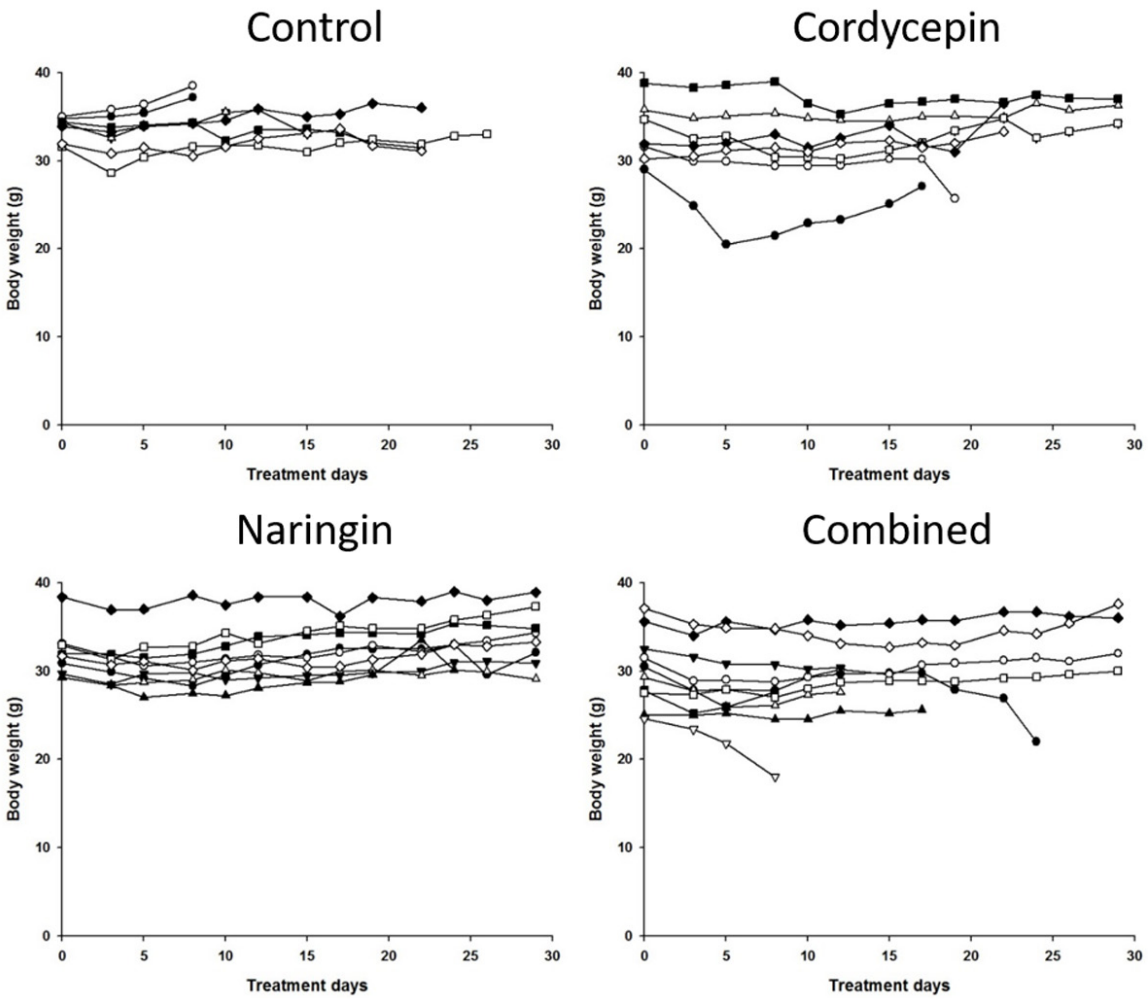

Figure S3. Body weight changes in the xenograft mice after the treatment of PEG, cordycepin, naringin, and the combination between cordycepin and naringin. The body weight of the xenograft mice was recorded before every treatment. The mice treated with PEG and naringin did not lose their weight in thirty days of treatment. In the cordycepin treatment group, one mouse lost body weight at twenty days of treatment. Two mice in the combined treatment group lost their body weight at eight and twenty-four days after treatment, respectively.

Table S1. Complete blood cell count (CBC) and serum biochemistry of the xenograft mice (N = 4 in each group)

Items	Control	Cordycepin	Naringin	Combined
CBC				
RBC (M/μL)	9.37 ± 0.25	8.25 ± 0.13	9.14 ± 0.31	8.34 ± 0.18
HGB (g/dL)	14.6 ± 0.6	12.6 ± 0.2	13.9 ± 0.2	12.05 ± 0.05
HCT (%)	43.1 ± 1.1	42.2 ± 0.9	43.7 ± 1.3	40.4 ± 0.1
MCV (fL)	48.6 ± 2.2	51.5 ± 2.8	47.8 ± 2.1	48.45 ± 0.95
MCH (pg)	15.4 ± 0.4	15.3 ± 0.0	15.2 ± 0.4	14.5 ± 0.4
MCHC (g/dL)	30.25 ± 0.21	29.85 ± 0.15	31.82 ± 0.20	29.8 ± 0.20
RET (K/μL)	369 ± 21.4	368.75 ± 20.5	418.6 ± 35.2	524.5 ± 50.8
RET (%)	4.21 ± 0.27	4.47 ± 0.18	4.58 ± 0.13	6.31 ± 0.75
PLT (K/μL)	800 ± 220	543 ± 160	1277 ± 251	1256 ± 150
WBC (K/μL)	6.8 ± 1.7	5.5 ± 2.2	5.63 ± 2.3	4.71 ± 0.70
NEUT (K/μL)	3.5 ± 0.6	2.1 ± 1.5	3.1 ± 1.6	2.1 ± 1.0
LYMPH (K/μL)	2.5 ± 0.9	3.1 ± 0.5	2.2 ± 0.8	2.2 ± 0.4
MONO (K/μL)	0.51 ± 0.32	0.29 ± 0.2	0.23 ± 0.41	0.38 ± 0.13
EO (K/μL)	0.24 ± 0.13	0.07 ± 0.03	0.15 ± 0.04	0.1 ± 0.01
BASO (K/μL)	0.25 ± 0.11	0.01 ± 0.02	0 ± 0.01	0.10 ± 0.03
NEUT (%)	58.3 ± 10.6	32.3 ± 15.1	51.1 ± 16.5	41.5 ± 14.7
LYMPH (%)	40.3 ± 8.2	61.5 ± 16.0	41.5 ± 11.7	48.8 ± 16.1
MONO (%)	4.0 ± 0.6	4.9 ± 1.0	4.2 ± 0.3	7.7 ± 1.5
EO (%)	1.3 ± 0.4	0.2 ± 0.1	2.6 ± 0.3	2.1 ± 0.4
Biochemistry				
ALT (U/L)	39.7 ± 26.1	39.5 ± 12.5	42.0 ± 15.5	49.5 ± 10.5
Alb (g/L)	31.2 ± 3.2	29.1 ± 1.1	30.2 ± 2.0	26.9 ± 0.4
Crea (mg/dL)	0.1 ± 0.1	0.4 ± 0.2	0.4 ± 0.3	0.6 ± 0.4
Glu (mg/dL)	187.7 ± 35.9	221.5 ± 18.9	212.6 ± 16.7	263.0 ± 11.4
AST (U/L)	86.7 ± 36.7	169.9 ± 58.2	112.1 ± 42.6	361.9 ± 252.9
T-Cho (mg/dL)	118.2 ± 35.7	107.2 ± 21.7	119.8 ± 10.8	92.8 ± 7.9
Na (mmol/L)	140.7 ± 1.3	142.1 ± 2.6	145.2 ± 1.4	139.5 ± 1.5
K (mmol/L)	7.2 ± 0.4	7.7 ± 0.2	7.7 ± 0.3	7.3 ± 0.1
Cl (mmol/L)	106.2 ± 0.8	109.7 ± 0.4	108.5 ± 0.8	108.4 ± 1.4

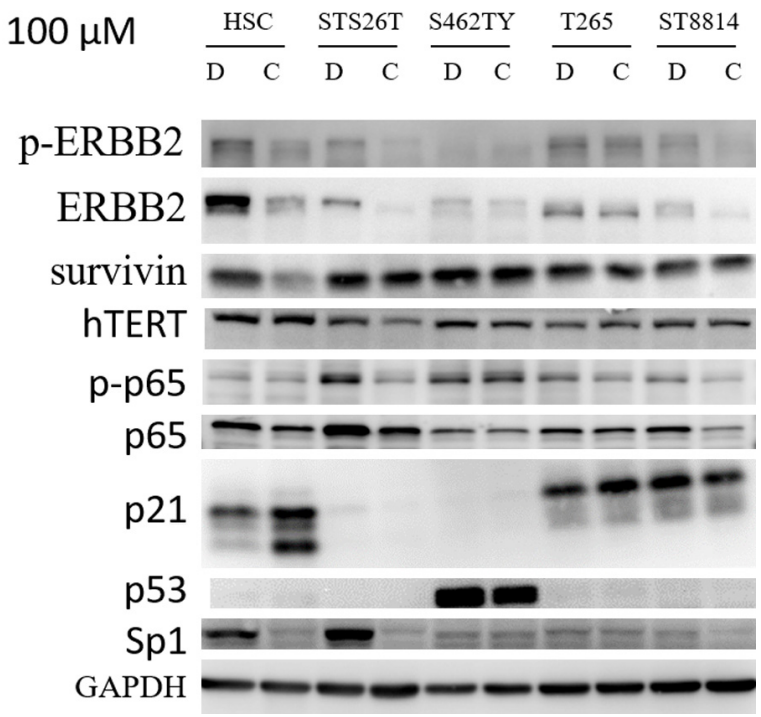

Figure S4. Immunoblotting for the specific protein levels in MPNST cells after treatment with 100 μM of cordycepin.